Estimating the Steric Sea Level Rise in Indonesian Seas using an Oceanic General Circulation Model

Sofian, I.,[1] Wijanarto, A.[2] and Karsidi, A.[3]
Geospatial Information Agency, Jl. Jakarta-Bogor KM 46, Cibinong 16911, Indonesia
E-mail: ibnusofian@gmail.com[1], wijanarto_ab@yahoo.com.au[2], akarsidi@gmail.com[3]
Phone: +62-21-8752062 Fax: +62-21-8752064

Abstract
The steric sea level rise rate in the Indonesian Seas was estimated using the HYbrid Coordinate Ocean Model (HYCOM). The HYCOM-estimated global steric sea level rise agrees well with the previous research results. The model result shows the thermosteric sea level rise is roughly 30% of the total sea level rise observed using altimeter. The steric sea level rise is approximately 20mm from 1993 when the total sea level rise reaches 58mm. The HYCOM results show high correlation coefficients (CC) with altimeter over the Indonesian Seas, with an average of more than 0.8. On the other hand, the contribution of ice melting (CIM) was also estimated using the HYCOM. The HYCOM modeled-CIM is investigated by subtracting the steric sea level rise from the total sea level rise observed using altimeter. The modeled contribution of ice melting (CIM) is ranging from 0.2 to 1.2cm/yr. Moreover, the projection of CIM shows that CIM is 16±2cm, 27±3cm, 41±4cm and 51±5cm in 2030, 2050, 2080 and 2100, respectively. Finally, if the temperature raises to more than 2°C, the thermosteric sea level rise will be 40cm to 80cm, in 2100. Thus, the total sea level rise will be more than 1m, and can reach to approximately 2m in 2100.

1. Introduction

Sea level rise is one of the most potentially serious impacts of global warming and climate change. The sea level rise, however, cannot be projected with high confidential level using the physical models due to dynamics of ice sheets and glaciers and to a lesser extent of the oceanic heat uptake that is not sufficiently understood (Vermer and Rahmstorf, 2009). Moreover, Vermeer and Rahmstorf (2009) also explained that the limited understanding was seen, e.g., in the fact that observed sea-level rise exceeded the predicted ones by models (best estimates) by ≈50% for the periods 1990–2006 and 1961–2003. Eventually, Intergovernmental Panel On Climate Change (IPCC) assessment report did not include rapid ice flow changes in its projected sea-level ranges, arguing that they could not yet be modeled, and consequently did not present an upper limit of the expected rise (IPCC, 2007). The mass balance of the ice sheets is a topic of considerable interest in the context of global warming and sea level rise. If totally melted, Greenland and West Antarctica would raise sea level by approximately 7m and 3m to 5 m, respectively. Thus, even a small amount of ice mass loss from the ice sheets would produce substantial sea level rise, with adverse societal and economic impacts on vulnerable low-lying coastal regions (Cazenave and Llovel, 2010). The IPCC projection is based upon the mass difference of ice melted and ice formed. Since the mass of the melting ice is bigger than that of the ice forming, Greenland ice sheet does contribute to the rise of sea level (Ridley et al., 2005). On the contrary, Antarctica is projected to freeze more and undergo increased ice forming, thus the ice forming in Antarctica and the ice melting in Greenland will cancel each other, with no net contribution to the sea level rise. Thus most of the contribution to the changing mass (the difference between ice melted and ice formed) is limited to the melting of glaciers and mountain ice cover (Meehl and Stocker, 2007). Rahmstorf (2007) used the relationship between the rise of the sea level and surface temperature to predict the sea level rise in the end of the 21st century. His estimate ranges from 50 cm to 140 cm, relative to the sea level in 1990. This prediction is higher than the projection of IPCC 4th Assessment Report (AR4). Moreover, the sea level rise before 1990, due to mass changing, is purely dominated by the glacial melting (Bindoff et al., 2007), thus Rahmstorf (2007)'s prediction excludes the changing of sea level due to the ice melting in Antarctica and Greenland.

Abdalati (2006) argued that the glaciers and ice sheets of the world contain enough ice to raise sea level by approximately 70m if they were to disappear entirely, and most of this ice is located in the climatically sensitive polar regions. Fortunately changes of this magnitude would probably take many thousands of years to occur, but recent discoveries indicate that these ice masses are responding to changes in today's climate more rapidly than previously thought (Abdalati, 2006). To avoid the impact of ice melting, Bryan (1996) calculated the thermosteric sea level rise using the ocean model. The model results explained that average rise in sea level of approximately 15±5cm by the time atmospheric carbon dioxide doubles for 80 years model running. Furthermore, the thermosteric and halosteric sea level rise from 1955 to 2003 are estimated to be 0.31±0.07mm/yr and 0.04±0.01mm/yr, respectively (Ishii et al., 2006). Due to the high sea level rise in the Indonesian Seas (Sofian, 2010), the estimation of contribution of ice melting (CIM) is inevitable to project the sea level rise in the future. The CIM estimation is conducted using the nested HYbrid Coordinate Ocean Model (HYCOM) on the global model. The nested HYCOM has the spatial resolution of 12.5km, while the global model has 50km of spatial resolutions.

2. Altimetry Data and Model Configuration

2.1 Altimetry Data

The satellite altimeter is commonly used to observe the sea surface height. The range between the satellite and the sea surface is measured at two different microwave frequencies. The orbit height is determined by using precision orbit determination techniques (Tapley, 1994). An uncorrected sea level measurement is calculated by subtracting the altimeter range from the orbit height, thereafter. The altimeter-derived sea level is constructed by applying corrections for atmospheric delay, sea state, inverted barometer, solid earth and ocean tides (Chelton et al., 2001). For TOPEX/Poseidon (T/P) (and now Jason-1 and 2) the point-to-point accuracy of these measurements has been shown to be 2 to 3 cm (Chelton et al., 2001). The merged product of MADT (Map of Absolute Dynamic Topography) is based on TOPEX/Poseidon (T/P), European Remote Sensing Satellite (ERS), GeoSat Follow On (GFO) and Envisat-derived sea surface height. A mapping procedure using optimal interpolation with realistic correlation functions is applied to produce MADT at a given date. The procedure generates one map for each altimeter mission but also a combined map merging measurements from all available altimeter missions (Le Traon and Ogor, 1998 and Ducet et al., 2000). The ADT is calculated using the formula as follows:

$$ADT = SLA + MDT$$

Equation 1

Where ADT, SLA and MDT are absolute dynamic topography, sea level anomaly and mean dynamic topography respectively. The MDT corresponds to the Mean Sea Surface Height minus Geoid (AVISO, 2009). The spatial resolution of MADT data are 0.333° latitude and longitude.

2.1 Model Configuration

The HYbrid Coordinate Ocean Model (Bleck, 2002) is a primitive equation ocean general circulation model that evolved from the Miami Isopycnic-Coordinate Ocean Model (MICOM). HYCOM is designed to retain the advantages of isopycnic coordinates as much as possible in the open stratified ocean, but to transform into level (pressure) coordinates in un-stratified regions such as the surface mixed layer, and also transform to terrain-following (sigma) coordinates in the coastal ocean (Shaji et al., 2005). The fundamental equations used in the HYCOM are presented based on the HYCOM user manual (Bleck, 2001). Further details of the HYCOM equations and numerical algorithms, along with a description and validation of the hybrid coordinate generator, can be found in Bleck (2002). The several vertical mixing choices embedded in HYCOM are described and initially evaluated by Halliwell (2004). He demonstrates that the K-Profile Parameterization (KPP and Large et al., 1994), NASA GISS level 2 turbulence closure, Malor-Yamada (MY) level 2.5 turbulence closure, and Price et al. (1986) dynamical instability model all perform reasonably well in low resolution climatic simulations. In an isopycnic system, the momentum equation can be described as follows:

$$\frac{\partial u}{\partial t} + \nabla\frac{u^2}{2} + (\varsigma + f)k \times u = -\nabla M - g\frac{\partial \tau}{\partial p}$$

Equation 2

Where ς, k, M, τ, and f are relative vorticity, vertical unit vector, Montgomery potential (geopotential), Reynold stress, and Coriolis parameter. The pressure deficit for the layer k can be expressed by the following equation:

$$\Pi_{k+1} = \Pi_k - g(\rho_{k+1} - \rho_k)\sum_{i=1}^{k}\langle h_k \rangle$$

Equation 3

Where Π,g,ρ, and h are pressure deficit, gravitation force, density, and water column height. In the moving ocean, the Montgomery potential M is equivalent to the potential Π established by the initial state. The Montgomery potential in layer k can be described as follows:

$$M_k = M_{k+1} + g(\rho_{k+1} - \rho_k)\sum_{i=1}^{k}(h_k)$$

Equation 4

In HYCOM, to model dissipation by bottom drag, the following equation is used:

$$\tau_b = C_d|\bar{u}_b|\bar{u}_b$$

Equation 5

Where C_d and $\bar{u}_b$ are drag coefficient, and average velocity in a slice of water of thickness δ_z (10m) situated just above the bottom. The residual velocity $\bar{c}$ is introduced by using the following equation.

$$D_{i,j} = C_d\left(\sqrt{\bar{u}_b^2 + \bar{v}_b^2} + \bar{c}\right)$$

Equation 6

In HYCOM, $\bar{c} = 10cm/sec$ and $C_d = 3 \times 10^{-3}$. The vertical divergence of the bottom-induced stress is calculated as:

$$\frac{\partial \tau_b}{\partial p} = \begin{cases} \frac{\partial \tau_{b_x}}{\partial p} \\ \frac{\partial \tau_{b_y}}{\partial p} \end{cases}$$

Equation 7

HYCOM is equipped with the two types of boundary conditions, the Newtonian relaxation in sponge layers (buffer zone), and full open-ocean boundary conditions. HYCOM contains a simple Newtonian relaxation scheme that can be used for sponge boundary zones, and relaxes to the climatology within any model subdomain. Temperature, salinity and vertical coordinate pressure levels within the relaxation boundary zones are updated for each time step. The nested model region is the Indonesian Sea including the Southern South China Sea, the Java Sea, the Sulawesi Sea, the Karimata Strait, and the Makassar Strait. The horizontal grid spans from 90°E to 140°E and from 15°S to 15°N (called IND, Indonesian Seas Domain), and the grid resolutions are Mercator 0.125° longitude and latitude. The model is configured with 26 layers, and the bottom topography is based on modified ETOPO2 data. The model uses KPP (K-Profile Parameterization) vertical mixing. The explanation of KPP and HYCOM equations and numerical algorithms can be found in Large et al., (1994) and Bleck (2002), respectively. The model relaxes to the World Ocean Atlas (WOA) 1998 monthly climatology that contains salinity and temperature profiles. IND is forced by the daily National Centers for Environmental Prediction (NCEP) reanalysis data, which includes wind stress, wind speed, surface air temperature, surface specific humidity, net shortwave and long wave radiations, and precipitation. The model's sea surface temperature (SST) is forced with daily sea surface temperature to obtain more realistic SST distributions. The IND is nested to the model which is configured with 26 layers, and setting up from 0°E to 360°E and from 75°S to 75°N with 0.5°longitude and latitude grid resolutions (called IPD, Indo-Pacific Ocean Domain). IPD uses the same topography data and parameter of forcing fields, initial conditions and mixing layer model as used in the IND. The summary of the IND model configuration can be seen in Table 1.

Table 1: IND model configuration

No	Parameter	Description	Comments
1	Geographical area	90°E to 140°E and from 15°S to 15°N	
2	Operational mode	Hind-cast	
3	Model run	from 1 January 1993 to 31 December 2010	Daily
4	Nesting conditions	on	IPD
5	Grid size	401 x 241	
6	Spatial resolutions	12.5 km x 12.5 km	
7	Layer	26 layers	
8	Time step baroclinic	180 seconds	
9	Time step barotropic	9 seconds	
10	Relaxation	WOA 1998	
11	Forcing fields	NCEP reanalysis II	Daily
12	Topography	ETOPO 2	
13	Vertical mixing model	KPP	
14	Tidal forcing	off	
15	River forcing	off	
16	SST forcing	NOAA high resolution daily SST	Daily

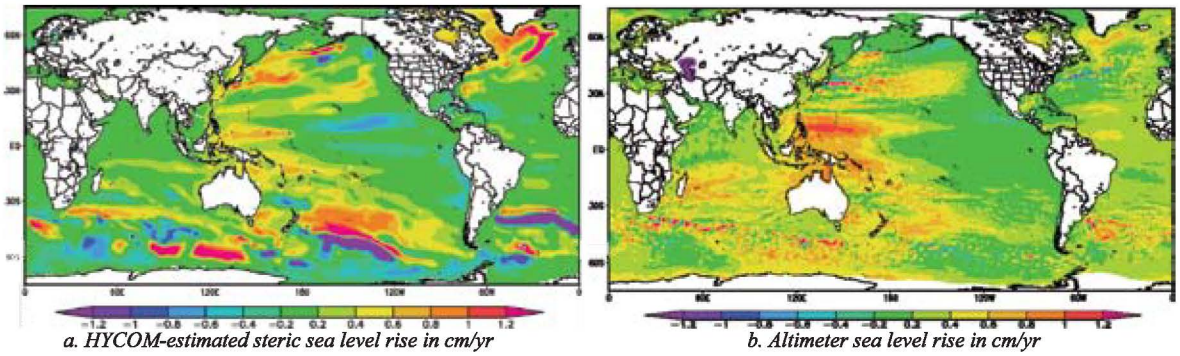

a. HYCOM-estimated steric sea level rise in cm/yr *b. Altimeter sea level rise in cm/yr*

Figure 1: Spatial distribution of steric and total sea level rise from 1993 to 2010

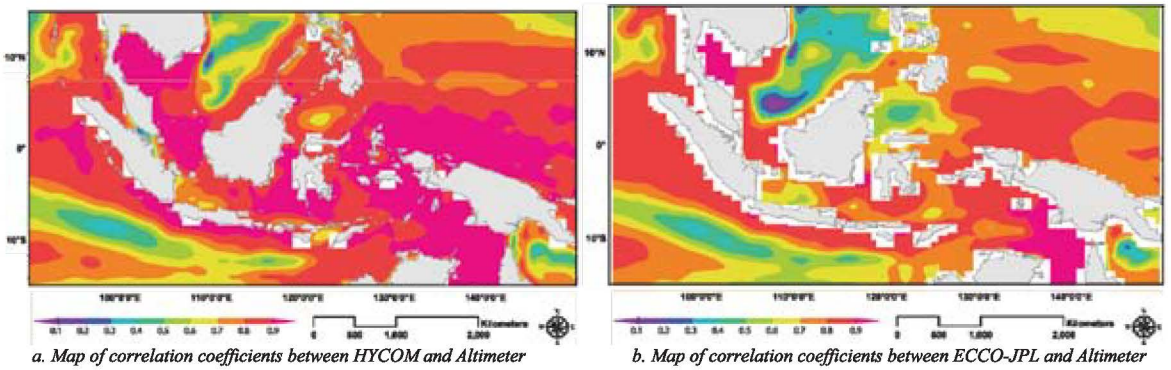

a. Map of correlation coefficients between HYCOM and Altimeter *b. Map of correlation coefficients between ECCO-JPL and Altimeter*

Figure 2: Spatial distribution of correlation coefficients (CC) between model and altimeter MADT

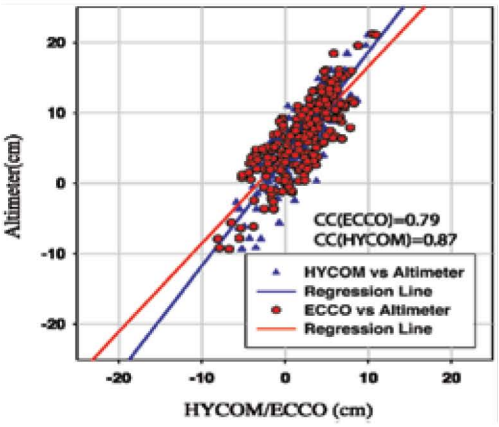

Figure 3: Scatter plot and regression analysis results between regionally averaged modeled-sea level and altimeter, from 90°E to 150°E and from 15°S to 15°N.

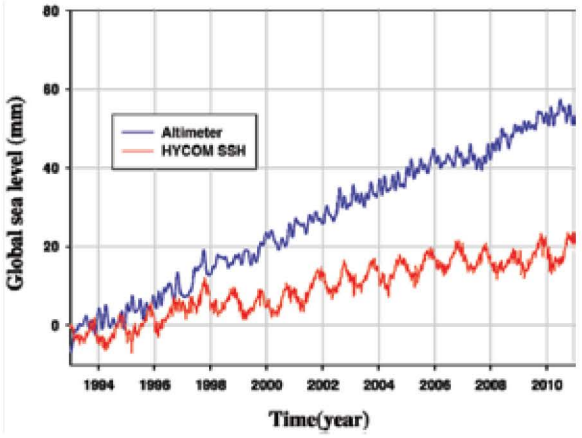

Figure 4: Global and steric sea level rises from 1993 to 2010, based on HYCOM-estimated sea level and altimeter, respectively

2.2 Model Validation

The altimeter ADT is used for the model validation. The CC between regionally averaged sea level from 90-150°E and from 15°N to 15°S both from HYCOM and ECCO against altimeter is illustrated in Figure 1. The HYCOM-estimated sea level shows higher CC than ECCO. The CC between models and altimeter are 0.87 and 0.79 for HYCOM and ECCO, respectively. The model validation results in the Indonesian Seas are shown in Figures 2 and 3.

HYCOM shows high correlation with altimeter, although some were moderately correlated in the Indian Ocean, southern part of South China Sea and south of Papua with the average CC of more than 0.8. The relationship between ECCO-JPL (Estimating the Circulation and Climate of the Ocean–Jet Propulsion Laboratory) NASA and altimeter is moderate to high, lower than one between HYCOM and Altimeter. Based on these validation results, it indicates that the HYCOM model is suitable to estimate the steric and ice melting impact on the sea level rise.

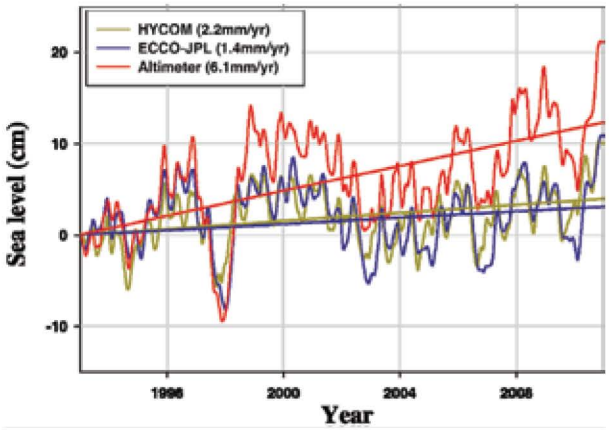

Figure 5: Time-series of altimeter and model-estimated sea levels

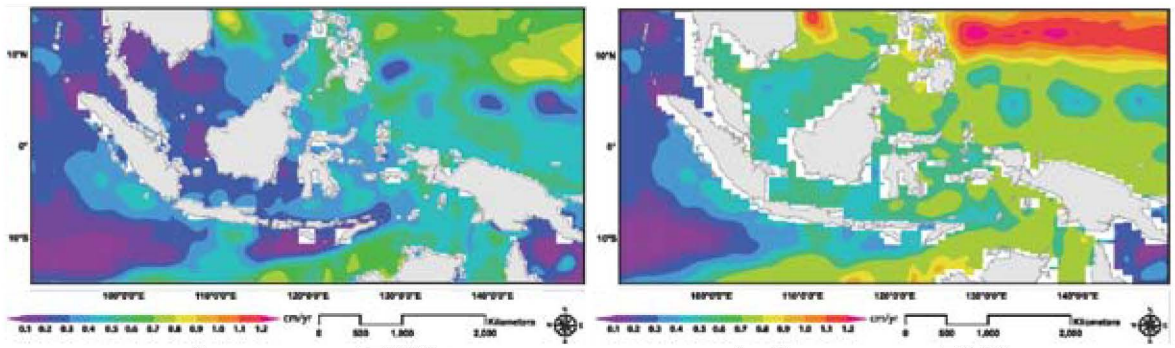

a. Altimeter minus HYCOM *b. Altimeter minus ECCO*

Figure 6: The spatial distribution of CIM rate based on HYCOM and ECCO

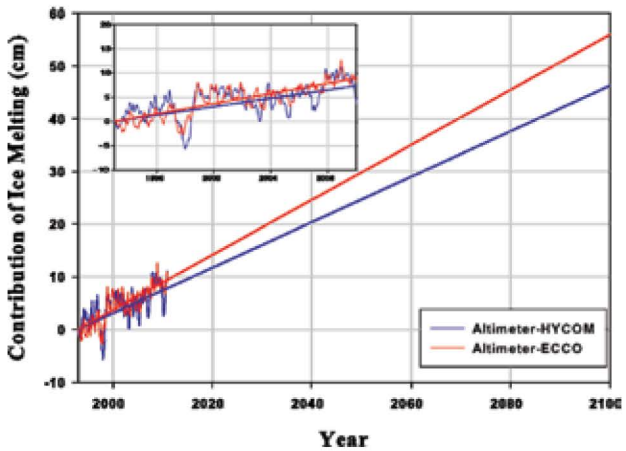

Figure 7: The projection of CIM until 2100 based on the altimeter and model

3. Results and Discussion

The recent thermosteric sea level rise calculated using HYCOM is depicted in Figure 4. The thermosteric sea level rise is roughly 30% from the total sea level rise observed by altimeter (AVISO, 2009). The steric sea level rise is approximately 20mm from 1993 when the total sea level rise reaches to 58mm. This fact indicates that ice melting contributes more than 60% of the total sea level rise. Cabanes et al., (2001) also reported that the thermosteric sea level rise from 1993 to 1998 was about 3.2±0.2mm/yr. Moreover, Antonov et al., (2005) argued that thermal expansion of the ocean from 0m to 700m deep contributed approximately 0.33mm/yr to global sea level rise from 1955 to 2003, with the thermosteric sea level rise 1.23mm/yr from 1993 to 2003 observed from altimeter. These previous research results are comparable with the HYCOM-estimated steric sea level rise, which is 1.18mm/yr, from 1993 to 2010. The spatial distribution of steric and global sea level rise is illustrated in Figure 1. Both steric and total sea level rises show that the highest sea level rises occurred in the tropical region from 30°S to 30°N. This result is similar with Ishii et al., (2006) that the thermal expansion averaged of the all ocean region from 60°S to 60°N is almost a half of the recent sea level rise. Eventually, the model-estimated steric sea level rise in Indonesia is ranging from -0.2 - 0.6cm/yr. The time-series of regionally averaged sea level (from 90 - 150°E and from 15°S to 15°N) is depicted in Figure 5. The sea level trends are 2.2mm/yr, 1.4mm/yr and 6.1mm/yr estimated by HYCOM, ECCO-JPL and altimeter, respectively. However, the sea level characteristics are similar between altimeter and model from 1993 to 1998 (Figure 5). This may indicate that sea level rise for this period is mainly caused by the steric sea level rise. Nevertheless, the altimeter is getting higher than modeled sea level from 1999 to 2010. As results, the altimeter sea level in 2010 rises more than 12cm relative to the sea level in 1993, while the model estimated steric sea level increases only 3±1cm. In general, the acceleration of CIM is highly influenced by the temperature rises, both ocean and air temperature. However, besides resulting in ice loss in Greenland and Antarctica, the increase of the surface temperature that causes this ice melting will reduce the area of ice-covered surface and will increase the absorption of the sun's short wave by the land and sea. This, in turn, will cause a positive albedo feedback that will accelerate the rate of global warming, which will increase the rate of ice-loss in Greenland and Antarctica. Increasing of global warming intensity will cause the increasing of sea level rise rate by the thermosteric process. The CIM is estimated by subtracting the steric sea level rise from the total sea level rise that observed using altimeter. The addition of sea level rise by ice melting was approximately 0.4mm/yr (observed from 2002 to 2005) (Velicogna and Wahr, 2006) and 0.25mm/yr (observed from 1993 to 2003) (Abdalati, 2006) from the Antarctica and the Greenland, respectively. The ice melting in Greenland occurred since the mid 1990s, and accelerated by increasing of time. Even though the ice elevation on highlands keeps increasing due to the snow, the ice melting in coastal areas and lowland is much greater and more intensive. The rate of ice melting in Greenland reached 100 Giga tons per year (Gt/year) by the end of 1990s, increasing to an observed rate of 200 Gt/year by 2006. (Approximately 360 Gt of ice melting is equivalent to a 1 mm increase in sea level.) The rate of ice mass change in Antarctica reached 80 Gt/year during the 1990s, and increased to 130 Gt/year by 2006 (UNEP/GRID-ARENDAL, 2007). The spatial distribution of CIM rate in the Indonesian Seas both estimated by HYCOM and ECCO are shown in Figure 6. Both HYCOM and ECCO show the similar pattern of CIM rate. Although, the HYCOM-estimated CIM rate is lower than the one estimated by ECCO. Furthermore, the CIM rate is ranging from 0.2cm/yr to 1.2cm/yr, both from HYCOM and ECCO. The highest CIM rate is occurred in the Pacific Ocean north of Papua Island, and the lowest is occurred in the Indian Ocean west of Sumatera, south of Papua, south of Nusa Tenggara and the Karimata Strait. The projection of CIM is depicted in Figure 7. The projection of CIM based on the altimeter and models are 16±2cm, 27±3cm, 41±4cm and 51±5cm in 2030, 2050, 2080 and 2100, respectively. If the temperature raises more than 2°C, the thermosteric sea level rise will be 40cm to 80cm (IPCC, 2007) in 2100. Thus, the total sea level rise will be more than 1m, and can reach approximately 2m in 2100. Finally, this extreme sea level rise will lead to strengthening the flood risk and worsening the coastal erosion in the future.

References

Abdalati, W., 2006, Recent Changes in High-Latitude Glaciers, Ice Caps and Ice Sheets, *Weather-April 2006*, 61, 4, 95-101.

Antonov, J. I., Levitus, S. and Boyer, T. P., 2005, Thermosteric Sea Level Rise, 1955–2003, Geoph. Res. Lett, Vol. 32, L12602, 1-4.

AVISO, 2009, Ssalto/*Duacs* User Handbook : (M)*SLA* and (M)*ADT* Near-Real Time and Delayed Time Products, *SALP-MU-P-EA-21065-CLS*, Edition 1.10.

Bindoff, N. L., Solomon, S., Qin, D., Manning, M., Chen, Z., Marquis, M., Averyt, K. B., Tignor, M. and Miller, H. L., 2007, Observations: Oceanic Climate Change and Sea Level. In: Solomon S, et al. (eds.). *Climate Change 2007: The Physical Science Basis. Contribution of Working Group I to the Fourth Assessment Report of the Intergovernmental Panel on Climate Change*. Cambridge University Press, Cambridge, United Kingdom, 385-432.

Bleck, R., 2001, Formulation of the Horizontal Pressure Gradient Force (PGF) in Generalized Coordinates. HYCOM Consortium, 1-3.

Bleck, R., 2002, An Oceanic General Circulation Model Framed in Hybrid Isopycnic-Cartesian Coordinates. *Ocean Modelling*, 4, 55-88.

Bryan, K., 1996, The Steric Component of Sea Level Rise Associated with Enhanced Greenhouse Gasses: a Model Study, *Climate Dynamic*, 12, 545-555.

Cabanes, C., Cazenave, A. and Provost, C. L., 2001, Sea Level Rise during 40years Determined from Satellite and In-Situ Observations, *Science*, 294, 840-842.

Cazenave, A. and Llovel, W., 2010, Contemporary of Sea Level Rise. *Annual Review of Marine Science*, Vol. 2, 145-173.

Chelton, D. B., Ries, J. C., Haines, B. J., Fu, L. L. and Callahan, P. S., 2001, Satellite Altimetry, in *Satellite Altimetry and Earth Sciences*, edited by L. L. Fu and A. Cazenave, 1– 131, Academic, San Diego, Calif.

Ducet, N., Le Traon, P. Y. and Reverdin, G., 2000: Global High- Resolution Mapping of Ocean Circulation from the Combination of T/P and ERS-1/2. *J. Geophys. Res.*, 105, 19477-19498.

Halliwell, G. R., 2004. Evaluation of vertical coordinate and vertical mixing algorithms in the Hybrid-Coordinate Ocean Model (HYCOM). *Ocean Modeling,* Vol. 7, 285-322.

IPCC, 2007, Climate Change 2007: Synthesis Report, Cambridge University Press, Cambridge.

Ishii, M., Kimoto, M., Sakamoto, K. and Iwasaki, S., 2006, Steric Sea Level changes Estimated from Historical Ocean Subsurface Temperature and Salinity Analysis, *J. Oceanography*, 62, 155-170.

Large, W. G., McWilliams, J. C. and Doney, S. C., 1994, Oceanic Vertical Mixing: A Review and a Model with Nonlocal Boundary Layer Parameterization. *J. Rev. Geophysics*, 32, 363-403.

Le Traon, P. Y. and Ogor, F., 1998, ERS-1/2 prbit Improvement using TOPEX/POSEIDON: The 2 cm Challenge, *J. Geoph. Res.,* 103(C4), 8045-8057.

Meehl, G. A. and Stocker, T. F., 2007, Global Climate Projections. In: Solomon S., et.al. (eds.), *Climate Change 2007: The Physical Science Basis. Contribution of Working Group I to the Fourth Assessment Report of the Intergovernmental Panel on Climate Change*. Cambridge University Press, Cambridge, 747–845.

Price J. F., Weller, R. A. and Pinkel, R., 1986, Diurnal Cycling: Observations and Models of the Upper Ocean Response to Diurnal Heating, Cooling and Wind Mixing, *J. Geophys. Res.*, 91, 8411-8427. *J. Appl. Met. and Clim*. 46, 890-899.

Rahmstorf, S., 2007: A Semi-Empirical Approach to Projecting Future Sea-Level Rise. *Science*, 315, 368-370.

Ridley, J. K., Huybrechts, P., Gregory, J. M. and Lowe, J. A., 2005, Elimination of the Greenland Ice Sheet in a High CO2 Climate. *Journal of Climate*, Vol. 18, 3409-3427.

Shaji, C., Wang, C., Halliwell, G. R. and Wallcraft, A., 2005, Simulation of Tropical Pacific and Atlantic Oceans using a Hybrid Coordinate Ocean Model. *Ocean Modelling*, 9, 253-282.

Sofian, I., 2010, Scientific Basis: Analysis and Projection of Sea Level Rise and Extreme Climate. Roadmap of Mainstreaming Climate change Issue into National Development, Bappenas-GTZ, 1-46.

Tapley, B. D., 1994, Precision orbit determination for TOPEX/POSEIDON, *J. Geophys. Res.,* 99(C12), 24383 – 24404.

UNEP/GRID-ARENDAL, 2007, Global Outlook for Ice & Snow, UNEP

Velicogna, I. and Wahr, J., 2006, Measurements of Time Variable Gravity Show Mass Loss in Antarctica, *Science*, DOI: 10/1126/Science1123785 (online through Science Express)

Vermer, M. and Rahmstorf, S., 2009, Global Sea Level Linked to Global Temperature, PNAS, 106, 51: 21527-21532.